

Fuzzy object growth model for newborn brain using Manifold learning

Ryosuke Nakano, Syoji Kabashi, Kei Kuramoto, Yuki Wakata, Kumiko Ando,
Reiichi Ishikura, Tomomoto Ishikawa, Shozo Hirota, and Yutaka Hata

Abstract—To develop a computer-aided diagnosis system for neonatal cerebral disorders, some literatures have shown atlas-based methods for segmenting parenchymal region in MR images. Because neonatal cerebrum deforms quickly by natural growth, we desire an atlas growth model to improve the accuracy of segmenting parenchymal region. This paper proposes a method for generating fuzzy object growth model (FOGM), which is an extension of fuzzy object model (FOM). FOGM is composed of some growth index weighted FOMs. To define the growth index, this paper introduces two methods. The first method calculates the growth index from revised age. Because the growth index will be different from person to person even through the same age, the second method estimates the growth index from cerebral shape using Manifold learning. To evaluate the proposed methods, we segment the parenchymal region of 16 subjects (revised age; 0-2 years old) using the synthesized FOGM. The results showed that FOGM was superior to FOM, and the Manifold learning based method gave the best accuracy. And, the growth index estimated with Manifold learning was significantly correlated with both of revised age and cerebral volume ($p < 0.001$).

I. INTRODUCTION

THE neonatal cerebral disorders have possibility to reduce the cerebral function. Therefore, it is required to detect and cure in their early stage. And, it leads to improve the quality of life (QOL) for patients and also their family [1]. One of the diagnosis indexes of the neonatal cerebral disorders is deformation of the cerebral shape. For example, as for patients suffering from epilepsy, a lot of cases show a brain formation disorder [2].

Segmentation of brain region from magnetic resonance (MR) image is needed to quantify brain deformation. Some methods for automatic segmentation have been proposed. For example, Prastawa *et al.* proposed a method which segments the brain region using MAP estimation [3], and Xue *et al.* proposed a method of cortical segmentation using expectation-maximization (EM) algorithm [4].

We also have proposed a segmentation method using fuzzy object model (FOM) [6]. FOM [5] is an atlas model which gives a prior knowledge of brain position and shape. FOM is generated from training data composed of subjects' MR images. To synthesize the consistent FOM, the subjects group should be controlled. Because the newborn brain shape

deforms quickly by natural growth, we control the subjects by the revised age. The method improved the segmentation accuracy by using FOM. However, the accuracy will decrease when the FOM is applied to a subject whose brain growth age is out of the age group. In order to improve the applicability of the FOM based method, we desire a method of synthesizing growable FOM.

One of the methods of analyzing developing brain is to generate a growth model. Davis *et al.* have proposed a method of generating a growth model using subjects' age [7]. Because the growth rate of newborn children will be different from person to person even through the same age, Aljaber *et al.* have proposed a method of generating a growth model by applying Manifold learning to newborn brain images [8]. The method normalizes brain images and applies Manifold learning using the change amount of normalization. However, it is hard to apply the method to various subjects because the normalization method of newborn brain does not establish well. Thus, we desire another method which does not use normalization.

In this paper, we propose a fuzzy object growth model (FOGM) by extending the conventional FOM. The FOGM is defined as a growth index weighted FOM. To estimate the growth index, we first employ their revised age. And, we propose an estimation method of brain growth index by means of Manifold learning using few brain anatomical landmarks. To validate the proposed methods, we segment the brain region using FOM and FOGM, and evaluate the segmentation accuracy.

II. PRELIMINARIES

A. Manifold Learning

Manifold learning is a method of dimensionality reduction [8]. We use the Laplacian eigenmaps [9] which is one of the Manifold learning techniques. The Laplacian eigenmaps makes a neighbor graph in a high dimensional space and calculates a graph Laplacian of the neighbor graph to project into a low dimensional space.

Consider k points, a_1, \dots, a_k , in a high dimensional space, and corresponding points, v_1, \dots, v_k , in a low dimensional space. The Laplacian eigenmaps have 3 steps to find the correspondence of points between the high and the low dimensional spaces.

[Step 1] Calculate a weight between all combinations of points in the high dimensional space, and obtain a weight matrix W . W is defined by Eq. (1).

$$w_{i,j} = \exp(-\|a_i - a_j\|_2^2 / t) \quad (1)$$

t is a normalization parameter.

R. Nakano, S. Kobashi, K. Kuramoto are with Graduate School of Engineering, University of Hyogo, Himeji, Japan (e-mail: kobashi@eng.u-hyogo.ac.jp).

S. Kobashi, K. Kuramoto, Y. Hata are also with WPI Immunology Research Center, Osaka University, Suita, Japan.

Y. Wakata, K. Ando, R. Ishikura, S. Hirota are with Hyogo College of Medicine, Nishinomiya, Japan.

T. Ishikawa is with Ishikawa Hospital, Himeji, Japan.

Y. Hata is with Graduate School of Simulation Studies, University of Hyogo, Kobe, Japan.

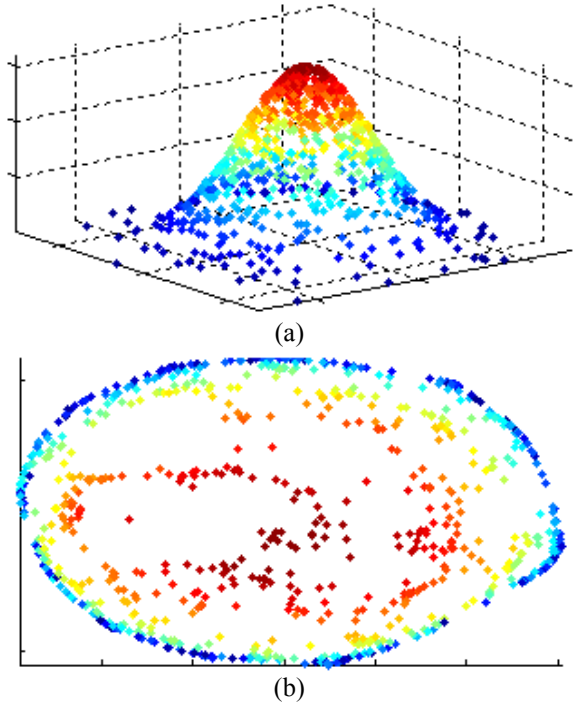


Fig. 1. Example of applying Manifold learning. (a) is 3D data which have Gaussian distribution shape. (b) is the result of manifold learning. 3D data is projected to 2D space while the positional relation of data is preserved.

[Step 2] Calculate a diagonal matrix $D_{i,i} = \sum_{j=1}^k W_{i,j}$, and calculate a graph Laplacian $L = D - W$.

[Step 3] Solve a generalized eigenvalue problem formulated by Eq. (2), and get non-zero eigenvalue λ . The eigenvector $v_{low} = [v_1, \dots, v_k]^T$ corresponding to the lowest eigenvalue λ_{low} shows corresponding points in the low dimensional space.

$$Lv = \lambda Dv \quad (2)$$

For example, we apply Manifold learning to 3-D data which have Gaussian distribution shape as shown in Fig. 1. It shows that 3-D data are projected to 2-D space while the positional relation of data is preserved.

B. Subjects and Materials

This study recruited 16 newborn subjects whose revised age was lower than 2 years old. The mean and standard deviation of the revised age was 122.13 ± 191.62 days. Revised age is defined as an age revised by normal fetal weeks (40 weeks) for premature babies. Their revised age, sex and number of slices are shown by table I. A volume is composed by slices. We had obtained informed consent from all their parents. According to diagnosis by radiologists, they had no significant cerebral disorders at the time of MR image acquisition.

We acquired T2-weighted MR images using 3.0T MR scanner (Intera, Philips Medical Systems) with a circularly polarized head coil as both the transmitter and receiver. T2-weighted MR images were acquired using the following parameters: echo time (TE) which is the necessary time till

TABLE I
DATA OF SUBJECTS

Data number	Sex	Revised age	Number of slices
1	M	3m3w	200
2	M	3w	130
3	M	4w	200
4	F	3m2w	220
5	M	2y	220
6	M	5w	180
7	F	10m3w	190
8	M	1w	120
9	M	0w	140
10	M	1m	140
11	M	2m	160
12	M	2m1w	170
13	M	0w	150
14	M	3m	190
15	F	0w	180
16	M	10m3w	200

M; male. F; female. y; year. m; month. w; week.

the signal was recognized was 106-165 msec; repetition time (TR) which is interval to give pulse was 2000 msec; slice thickness, 1.5 mm; space between slices, 0.75 mm; field of view (FOV) and number of slices were adjusted by a size of target head size (120 - 200 mm), image matrix is 320×320 voxel; resolution is $0.75 \times 0.75 \times 0.75 \text{ mm}^3$.

III. PROPOSED METHODS

The proposed method synthesizes FOGM using training dataset which is composed of MR images acquired from different subjects with various growth indexes. To estimate the growth index, we propose two methods. The first method calculates growth index from revised age. However, the neonatal cerebrum deformation by natural growth will be different from person to person, and the growth index will not same as the revised age. The second method proposes an estimation method of growth index using Manifold learning. We employ distances among brain anatomical landmarks to calculate a weight matrix among training data. To validate the performance of FOGM, we propose anatomical recognition method in neonatal brain MR images using FOM and FOGM. The flowchart of proposed method is shown by Fig.2.

In the following subsections, we describe the proposed FOGM in Section IIIA, two methods for estimating growth index for training datasets in Section IIIB, and Section IIIC shows growth index estimation method for evaluation data, and the anatomical recognition method.

A. Fuzzy Object Growth Model

FOGM is an extension of FOM [4]. FOM is defined by voxels, and each voxel has a fuzzy degree between 0 and 1. Fuzzy degree means a degree of belonging to a target region (*i.e.*, brain region) should be recognized. 1 fuzzy degree means that the position is completely inside the target region, and 0 fuzzy degree means that the position is completely outside the target region.

In contrast, each voxel of FOGM has a set of distances from the target contour for each training subject, and FOGM has a table of growth index of the training subjects. The method consists of 4 steps. FOGM is generated only once

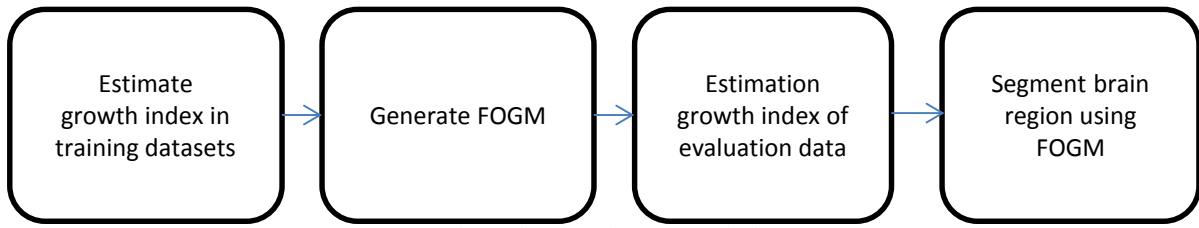


Fig. 2. Flowchart of propose method.

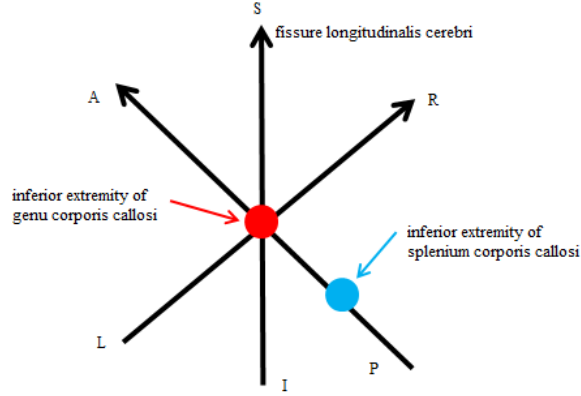


Fig. 3. Coordinate system for calibration of brain pose/position. A, anterior; P, posterior; S, superior; I, inferior; L, left and R, right.

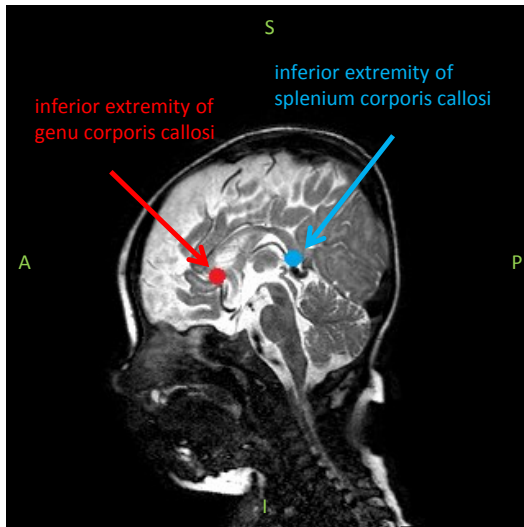


Fig. 4. Landmarks for calibration of brain pose/position. The red point is the inferior extremity of genu corpus calloso, and the blue point is the inferior extremity of splenium corpus calloso.

from the training subjects, and we do not need to generate FOGM again when analyzing evaluating subjects.

[Algorithm] FOGM generation

[Step 1] For each training subject, experts delineate the brain region in MR images manually.

[Step 2] Calibrate the pose/position of the brain region to a coordinate system because there is variability among subjects. The coordinate system used is illustrated in Fig. 3. The inferior extremity of genu corpus calloso is the origin. A line which connects the origin to the inferior extremity of splenium corpus calloso is anterior-posterior (AP) axis, and the line of fissure longitudinalis cerebri is superior-inferior (SI) axis. The

4	3	4	8	7	8
3	0	3	7	6	7
4	3	4	8	7	8

(a)

4	3	4	8	7	8
3	0	3	7	6	7
4	3	4	8	7	8

(b)

Fig. 5. 3-D Chamfer distance mask. (a) is used in the current slice. (b) is used in the previous and the next slice.

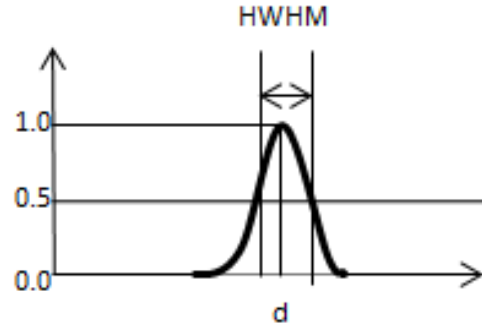


Fig. 6. Weighting function for calculate average and variance. This function has Gaussian distribution shape.

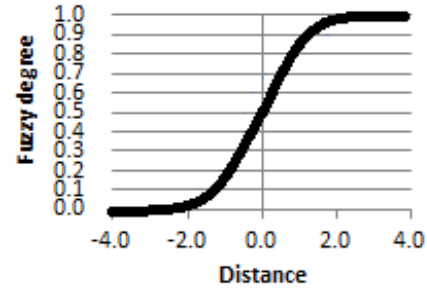


Fig. 7. Fuzzy membership function.

landmarks are detected manually, and are shown by Fig. 4.

[Step 3] For each voxel in all training data, calculate 3-D chamfer distance [10] (Figure 5) to the delineated brain surface. One voxel has a set of distances whose number is the same as the number of training data, n . At a voxel p , it is represented by $\mathbf{D}(p) = \{d_1(p), d_2(p), \dots, d_n(p)\}$.

[Step 4] Estimate growth index using methods described in subsection IIIB. It is represented by $\mathbf{v} = \{v_1, v_2, \dots, v_n\}$.

[End of algorithm]

After generating FOGM, the method synthesizes FOM at a certain growth index when analyzing an evaluation data. Consider a FOM generation whose growth index is v_i ($0 \leq v_i \leq 1$). We define a fuzzy degree for every voxel, p , as below.

First, it calculates weighted average and variance of distances at voxel p by;

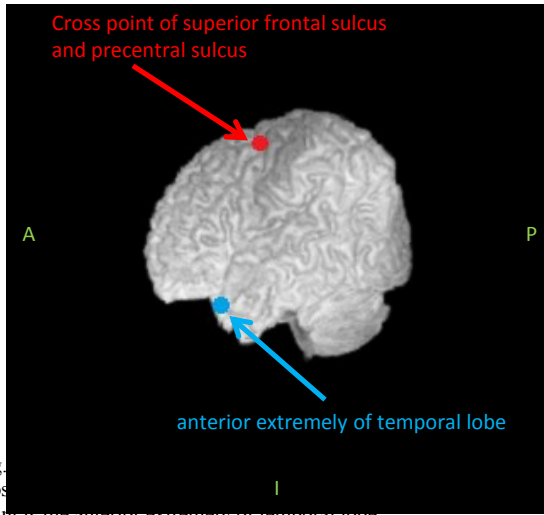


Fig. 6. The blue point is the anterior extremity of temporal lobe.

$$m(p) = \frac{\sum_{i=1}^N w_i \times d_i(p)}{\sum_{i=1}^N w_i} \quad (3)$$

$$\sigma^2(p) = \frac{\sum_{i=1}^N w_i (d_i(p) - \mu(p))^2}{\sum_{i=1}^N w_i} \quad (4)$$

$$w_i = e^{-\frac{(v_i - v_T)^2}{K}} \quad (5)$$

K is fuzzification parameter and has positive value. The shape of Eq. (5) is illustrated in Fig. 6. If K is the smaller, FOM is generated in the range of wider growth index. As K becomes the bigger, the range becomes the smaller. The relationship between K and half-width of half-maximum (HWHM) is

$$K = HWHM / \sqrt{2 \ln 2}. \quad (6)$$

The fuzzy degree at voxel p is calculated using weighted average $m(p)$ and variance $\sigma^2(p)$ by Eq. (7).

$$\mu(p) = \begin{cases} 0 & \text{if } m(p) \leq -\frac{1}{2}\sigma^2 \\ \frac{1}{2} \sin\left(\frac{m(p)}{\sigma^2} \pi\right) + \frac{1}{2} & \text{if } -\frac{1}{2}\sigma^2 < m(p) < \frac{1}{2}\sigma^2 \\ 1 & \text{if } m(p) \geq \frac{1}{2}\sigma^2 \end{cases} \quad (7)$$

When a voxel of interest is on the cerebral surface, the fuzzy degree takes 0.5. When the voxel leaves outside from the cerebral surface, the fuzzy degree will be smaller. And, the voxel comes inside the brain, the fuzzy degree will be bigger. That is illustrated in Fig. 7. The gradient is determined by the variance of distance. The variance becomes bigger, the gradient becomes gentle. In contrast, the variance becomes smaller, the gradient becomes steep.

B. Estimation of Growth Index in Training Datasets

This section introduces two methods for estimating growth index in the training data. The first method (**m1**) applies a liner conversion of the revised age as the growth index. The growth index of the oldest subject in data is 1, and the growth index of the youngest subject is 0. The growth index, v_T , of a subject whose revised age is y is defined by;

$$v_T = \max\left(\min\left(\frac{y}{y_{\max} - y_{\min}}, 1\right), 0\right) \quad (8)$$

TABLE II
ESTIMATION RESULTS OF GROWTH INDEX

Subject #	Truth value	Estimation Result	Error
1	0.5145	0.5132	-0.0012
2	0.3528	0.3486	-0.0042
3	0.1359	0.1488	0.0129
4	0.7331	0.8075	0.0744
5	1.0000	1.0000	0.0000
6	0.4654	0.4685	0.0031
7	0.8809	1.0000	0.1191
8	0.1350	0.0647	-0.0703
9	0.0000	0.0000	0.0000
10	0.2950	0.2840	-0.0110
11	0.2912	0.2801	-0.0111
12	0.4917	0.4923	0.0006
13	0.3275	0.3214	-0.0061
14	0.2246	0.1998	-0.0248
15	0.1687	0.1130	-0.0556
16	0.9412	1.0000	0.0588

where y_{\max} and y_{\min} are the oldest revised age and the youngest revised age in the training dataset, respectively.

The second method (**m2**) estimates the growth index by means of Manifold learning. Manifold learning calculates distances of all combination of training data in a high dimensional space, and resolves eigenvalue of graph Laplacian to project the training data to a low dimensional space.

At first, we manually detect N_p brain anatomical landmarks every each subject in training datasets. Next, the method calculates Euclidean distance between all combination of the detected landmarks. The calculated distances are used as a characteristic vector of the subject i , $\mathbf{a}(i) = \{a_1(i), a_2(i), \dots, a_M(i)\}$, where M is the number of distances and is $N_p C_2$. Using the characteristic vectors, $\mathbf{a}_1, \mathbf{a}_2, \dots, \mathbf{a}_k$, all subjects in the training dataset is assigned in a high dimensional space. The method calculates neighborhood relations between them using Eq. (1), and then solves a generalized eigenvalue problem to project the high dimensional data into 1 dimensional space.

The eigenvalues in the 1 dimensional space are normalized to a value between 0 and 1 by a liner conversion. We define the normalize value, v_1, \dots, v_k , as growth indexes of subjects in the training dataset. The maximum of growth index is 1, and the minimum is 0.

C. Estimation of Growth Index for Evaluation Data

In case of (**m1**), the growth index is estimated by Eq. (8) using revised age of the evaluating subject.

In case of (**m2**), the growth index is estimated as below. Generalized eigenvalue problem which is given by Eq. (2) can be transformed to Eq. (9) by multiplying D^{-1} to the both side.

$$D^{-1}Lv = \lambda v \quad (9)$$

When the number of subjects in the training datasets is N , $X = D^{-1}L$ is a square matrix of N rows and columns, and Eq. (9) can be transformed to

$$v_T = \sum_{i=1, i \neq T}^N X_{Ti} \times v_i / (\lambda - 1). \quad (10)$$

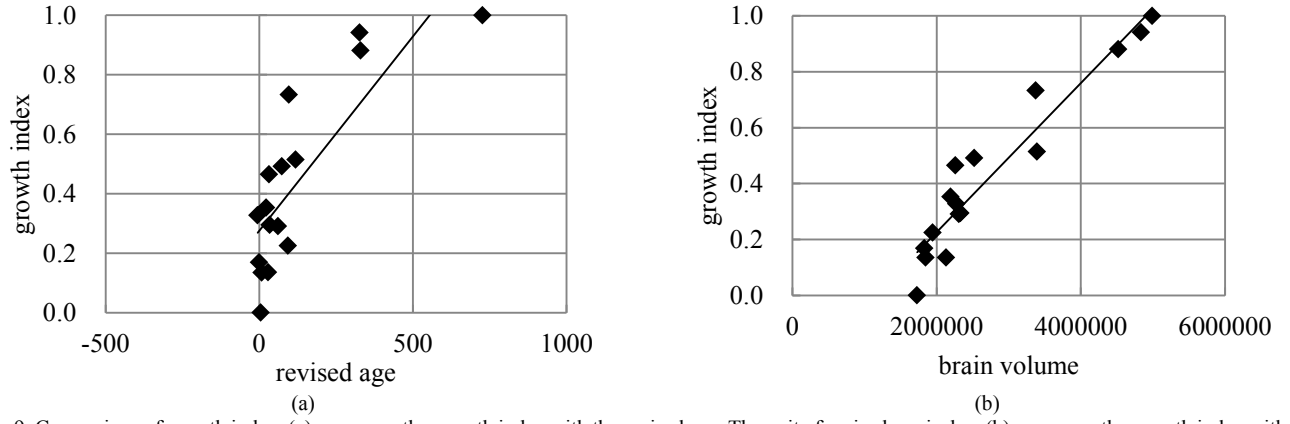


Fig. 9. Comparison of growth index. (a) compares the growth index with the revised age. The unit of revised age is day. (b) compares the growth index with the cerebral volume. The unit of brain volume is cc. The lines are regression lines.

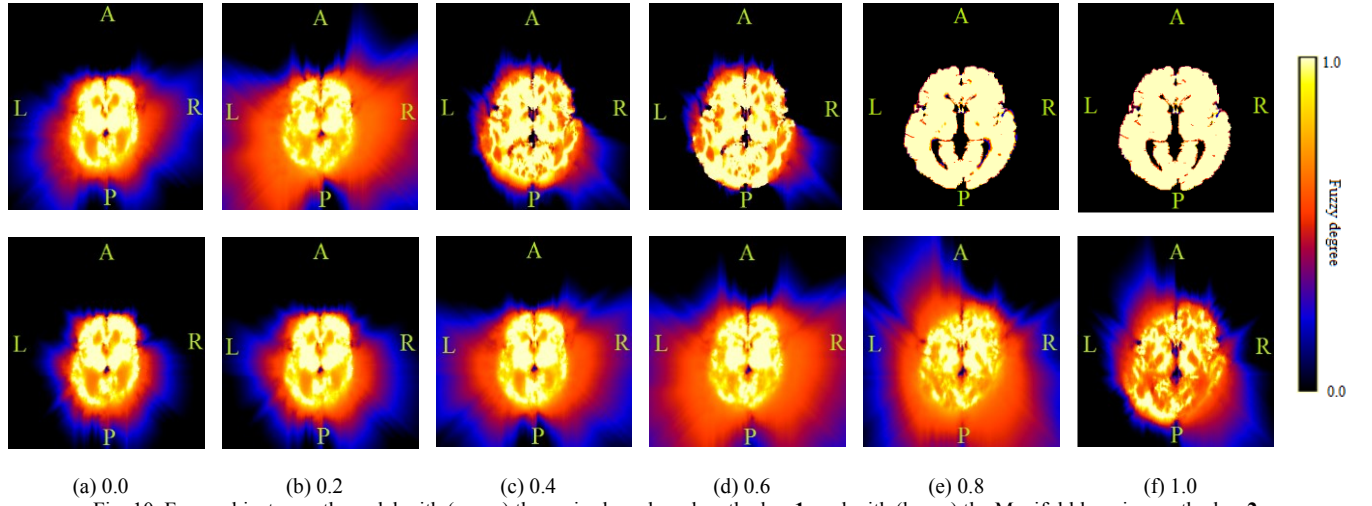


Fig. 10. Fuzzy object growth model with (upper) the revised age based method, **m1**, and with (lower) the Manifold learning method, **m2**.

where v_i and λ are gotten by Manifold learning for training data. W can be calculated by Eq. (1) using a characteristic vector of the evaluating subject and the vectors of training data. That is, the anatomical landmarks should be detected manually. Therefore, we can calculate D and L using W , and can estimate the growth index of the evaluating data.

D. Automated Anatomical Recognition of the Brain Region using Fuzzy Object Growth Model

To evaluate the proposed methods, we applied them to segmentation of the brain region. Although there are many image segmentation methods, we employ a simple method for evaluation of the proposed methods. The segmentation method consists of the following steps.

- [Step 1] Manually detect anatomical landmarks of the evaluation data.
- [Step 2] Estimate growth index of the evaluation data.
- [Step 3] Generate FOM at the growth index.
- [Step 4] Align the generated FOM to the evaluation data.
- [Step 5] Fuzzify the evaluation data by assigning a fuzzy degree of the aligned FOM to each voxel of evaluation data. It is called a fuzzy voxel map.
- [Step 6] Defuzzify the fuzzy voxel map by thresholding. For each voxel, if the fuzzy degree is higher than or equal to a

threshold, the voxel is labeled as target region, otherwise it is labeled as background.

IV. EXPERIMENTAL RESULTS

A. Growth index estimation by Manifold learning

We applied the Manifold based estimation method (**m2**) to 16 subjects which were shown by Table I. The brain anatomical landmarks used were the inferior extremity of genu corporis callosi, the inferior extremity of splenium corporis callosi, the right and the left cross points of the superior frontal sulcus and the precentral sulcus, the right and the left anterior extremity points of temporal lobe (See Fig. 4 and 8). They were selected because landmark detection in MR images was relatively easy. They were detected manually using multi-planer reconstruction (MPR) images by radiologist. The normalization parameter t of Eq. (1) was 5000.

We compared the estimated growth index with the revised age and with the cerebral volume for evaluating the performance as shown in Fig. 9. The cerebral volume was calculated by segmenting the cerebral region manually. Correlation coefficients were 0.814 and 0.956, respectively, and there are significant correlation ($p < 0.001$ for the

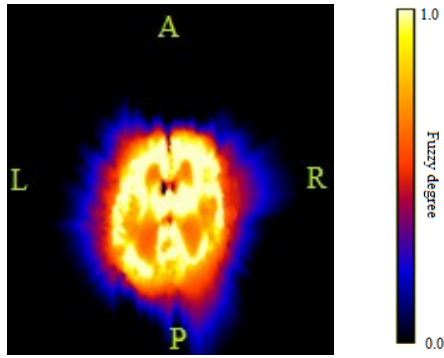


Fig. 11. Fuzzy object model with the previous method [6].

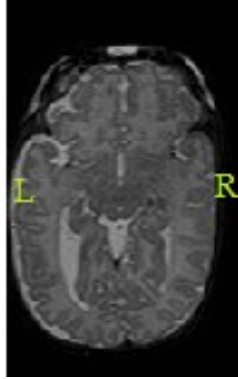


Fig. 12. Raw MR image. 160th image among 320 axial images of Subject 2.

revised age, $p < 10^{-8}$ for the cerebral volume). The results showed that the estimated growth index with Manifold learning is compatible to the revised age and the cerebral volume.

Next, we evaluated the estimation method for unknown data. We conducted a leave one out cross validation (LOOCV) test. We applied Manifold learning to all subjects excepting an evaluating subject. After that, we estimated a growth index of the evaluating subject. The truth values were a growth index estimated by Manifold learning using all data. The experimental results are shown in Table II. Mean absolute error (MAE) was 0.0283. Accuracies declined a bit for subjects whose growth indexes were close to the maximum (1.0) or the minimum (0.0). We are considering that the accuracy will be declined because it requires extrapolation for the subjects. Thus, we expect that the accuracy will be improved by increasing the number of training subjects.

B. Fuzzy Object Growth Model

We generated FOGM by applying the proposed two methods. The HWHM was experimentally determined, and was 0.1 for **m1**, and 0.2 for **m2**. The generated FOGMs are shown in Fig. 10. The results showed that the cerebrum becomes bigger with increasing the growth index. Figure 11 shows FOM generated by the previous method described in Ref. [6]. The method calculates fuzzy degrees of each voxel using the simple average, and selects 8 training subjects whose revised ages were under one month. In previous method, FOM has the shape which is almost an ellipse. In our methods, FOGM has recessed between frontal lobe and

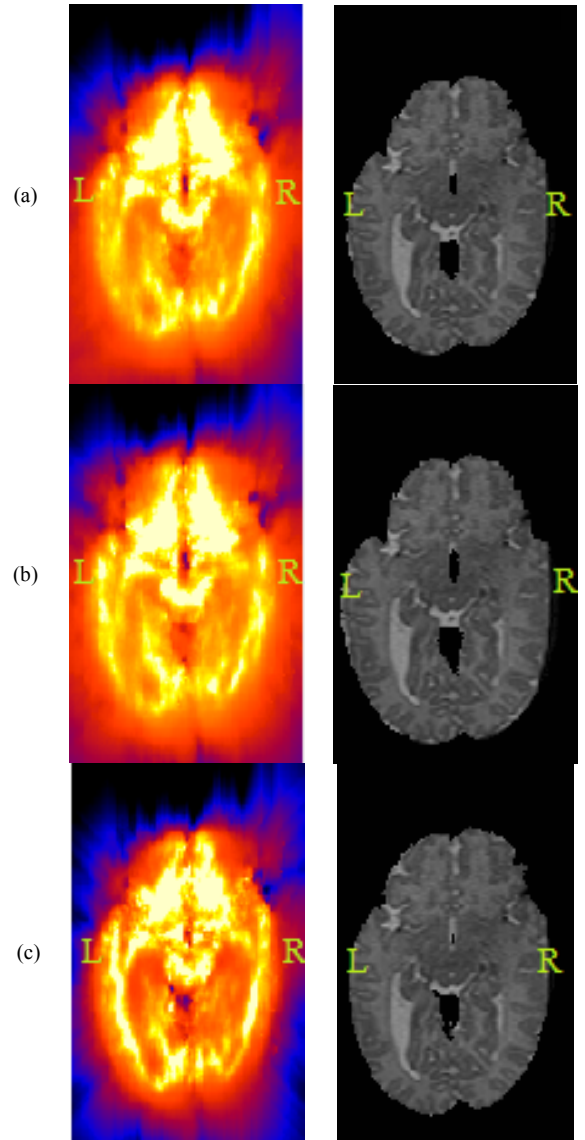


Fig. 13. Segmentation result for Subject 2. (a) are results of first method. (b) are results of second method. (c) are results of previous method. Left images are fuzzification result. Right images are segmentation result.

TABLE III
AUC OF SUBJECTS WHOSE REVISED AGES ARE UNDER A MONTH

Evaluating subject	Proposed method (m1)	Proposed method (m2)	Conventional method
2	0.99401	0.99367	0.99423
3	0.99245	0.99297	0.99272
6	0.97976	0.97910	0.97860
8	0.99123	0.99156	0.99076
9	0.99072	0.98965	0.99095
10	0.99037	0.99001	0.98753
13	0.98853	0.98716	0.98923
15	0.98862	0.98923	0.98503

temporal lobe.

To evaluate the effectiveness of the proposed methods, we segmented the cerebral region using the synthesized FOM. The conventional method [6] synthesized FOM using only subjects whose revised ages were under one month. To compare results among the proposed two methods and the

TABLE IV
AUC OF SUBJECTS WHOSE REVISED AGES ARE OVER ONE MONTH

Evaluating subject	Proposed method (m1)	Proposed method (m2)	Conventional method
1	0.96756	0.97082	0.97357
4	0.98552	0.98115	0.97124
5	0.96388	0.98007	0.95856
6	0.65280	0.89693	0.91574
11	0.98422	0.98532	0.98616
12	0.97605	0.97687	0.98028
14	0.98893	0.98660	0.98690
16	0.79145	0.97206	0.95551

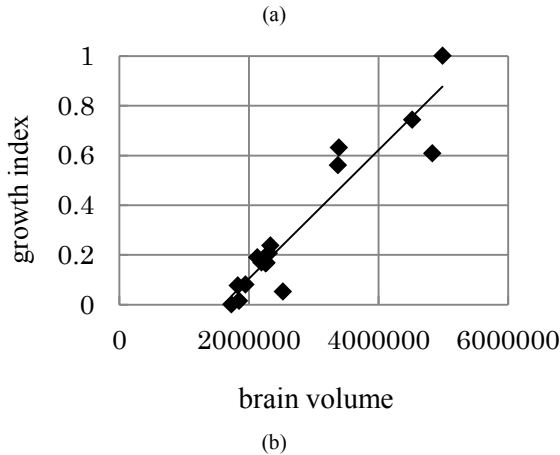
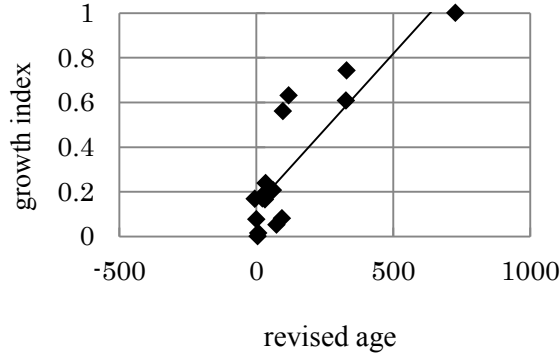


Fig. 14. Comparison growth index estimated by 4 points. (a) is the result of comparison between growth index and revised age. The unit of revised age is day. (b) is the result of comparison between growth index and brain volume. The unit of brain volume is cc. The lines are regression lines.

conventional method, we segmented the cerebral region for under one month subjects. Figure 12 shows a raw MR image, and Fig. 13 shows fuzzification results and the segmentation results. The threshold of defuzzification used was 0.5. The results show that all methods recognized the brain region well, however, there are some differences. The conventional method shown in Fig. 13 (c) tends to produce under-segmentation in the frontal edge of the temporal lobe, but the proposed methods shown in Fig. 13(a) and (b) segmented the region accurately.

To evaluate the segmentation results quantitatively, we calculated sensitivity and false positive volume fraction (FPVF). The ground truth was the result of manual segmentation. Because the accuracy was changed by the

TABLE V
RESULTS OF ESTIMATION GROWTH INDEX WITH THE 4 POINTS METHOD

Evaluating subject	Truth value	Estimation result	Error
1	0.63062	0.69402	0.06340
2	0.16888	0.16445	-0.00443
3	0.19006	0.19263	0.00257
4	0.56042	0.59063	0.03021
5	1.00000	1.00000	0.00000
6	0.16511	0.16123	-0.00388
7	0.74269	0.87860	0.13591
8	0.01519	0.00000	-0.01519
9	0.00000	0.00000	0.00000
10	0.23780	0.24087	0.00307
11	0.20696	0.20746	0.00050
12	0.05152	0.05612	0.00460
13	0.16801	0.16371	-0.00430
14	0.08040	0.05562	-0.02478
15	0.07657	0.04415	-0.03242
16	0.60749	0.65714	0.04965

TABLE VI
COMPARISON OF AUC WITH BETWEEN THE 6 POINTS METHOD AND THE 4 POINT METHOD

Evaluating subject	6 points	4 points
1	0.97082	0.98192
2	0.99367	0.98782
3	0.99297	0.99254
4	0.98115	0.98166
5	0.98007	0.98478
6	0.97910	0.98155
7	0.89693	0.92033
8	0.99156	0.99101
9	0.98965	0.98949
10	0.99001	0.99037
11	0.98532	0.98384
12	0.97687	0.97762
13	0.98716	0.98662
14	0.98660	0.96717
15	0.98923	0.98878
16	0.97206	0.96717

threshold parameter, we analyzed that by using a receiver operating characteristic (ROC) curve [11] while changing the threshold from 0 to 1. When FPVF is small, the accuracy is better if sensitivity is bigger. To quantify it, we calculated area under the curve (AUC) of the ROC curve. The AUC takes a value between 0% and 100%, the higher AUC means the better accuracy.

Table III tabulates AUC of each method, they were calculated by using LOOCV. LOOCV test generates FOGM using all 16 subjects excepting the evaluating subject. That is, all subjects including subjects whose revised ages were over one month were used for growth index estimation and FOGM generation. AUC (average \pm standard deviation) of the proposed method (m1) was 0.990 ± 0.004 , of the proposed method (m2) was 0.990 ± 0.005 , and of the conventional method was 0.989 ± 0.005 . The results showed that segmentation accuracies of the proposed methods were higher than the conventional method.

Next, we applied the methods to subjects whose revised ages were over one month in the same manner. The conventional method generated FOM using 8 subjects whose

revised ages were under one month. Table IV tabulates the calculated AUC. AUC (average \pm standard deviation) of the proposed method (**m1**) was 0.914 ± 0.124 , of the proposed method (**m2**) was 0.969 ± 0.030 , and of the conventional method was 0.966 ± 0.023 . The results for one month over subjects decreased than those for one month less subjects shown in table III. The decrease amount of the proposed method (**m2**) was the smallest among them. The results concluded that the Manifold learning based method (**m2**) shows the best performance for any age group.

V. DISCUSSIONS

The Manifold learning based (**m2**) method estimates growth index by using some anatomical feature points. There is a possibility that the estimation accuracy will depend on the number of feature points. In order to validate that, we evaluate the performance by the proposed method by using 4 feature points; inferior extremity of genu corporis callosi, inferior extremity of splenium corporis callosi, right and left of cross point of superior frontal sulcus and precentral sulcus. The normalization parameter t of Eq. (1) was 1000. And, HWHM of Eq. (6) was 0.3. Those parameters are experimentally determined.

Figure 14 compares the estimated growth index with the revised age and with the brain volume. Correlation coefficients were 0.861 and 0.943 respectively. There are significant correlation ($p < 0.001$ for the revised age, $p < 10^{-8}$ for the brain volume). Also, we conducted LOOCV test for growth index estimation and cerebral region segmentation. Comparison of the results between 4 points and 6 points are shown in Table VI and Table V. MAE of growth index estimation with the 4 points method was 0.0238, and with 6 points method was 0.0283. The results show that there are not large differences of accuracy between the 4 points method and the 6 points method. Therefore, the proposed method gives a good performance even if less feature points. It will be good for users to decrease the number of required input points

VI. CONCLUSION

This paper has introduced FOGM which is an atlas model deformed by natural growth. And, it proposes two methods for estimating growth index. The first method (**m1**) estimated the growth index from the revised age. The second method (**m2**) estimated that by means of Manifold learning using anatomical feature points. The estimation results with **m2** showed a significant correlation with the brain volume and with the revised age. And, it estimated growth index of unknown subject with a good accuracy (MAE of 0.0283).

To validate the performance of FOGM, the proposed methods were applied to brain segmentation. The results concluded that the use of FOGM and growth index estimation with Manifold learning improved the segmentation accuracy. And, the Manifold learning method could be applied to large range of age. The performance of the proposed method was not changed when decreasing to 4 feature points. We used a threshold processing as segmentation method in this paper to evaluate only the performance of the proposed method. We

expect that the accuracy of segmentation will increase by using the other solicited method such as fuzzy connected image segmentation [6].

Future work is to increase the number of subjects in order to investigate the performance of the proposed methods, and to consider an analysis parameters, parameter t in Eq. (1) and HWHM in Eq. (6).

REFERENCES

- [1] A. Hashioka, S. Kobashi, K. Kuramoto, Y. Wakata, K. Ando, R. Ishikura, T. Ishikawa, S. Hirota and Y. Hata, "Shape and Appearance Knowledge Based Brain Segmentation for Neonatal MR Images," Proc. of 2012 World Automation Cong., online, 2012.
- [2] S. Sanada, E. Oka, S. Ohtahara, M. Kawahara, K. Sakae and Y. Hiraki, "Cerebral dysgenesis and psychomotor retardation in neonatal epilepsy," Journal of Okayama Medical Association, Vol. 109, No. 1, pp.1-6, 1997.
- [3] M. Prastawa, J. H. Gilmore, W. Lin and G. Gerig, "Automatic Segmentation of MR Images of Developing Newborn Brain," Medical Image Analysis, Vol. 9, No. 5, pp. 457-466, 2005.
- [4] H. Xue, L. Srinivasan, S. Jiang, M. Rutherford, A. D. Edwards, D. Rueckert and J.V. Hajnal, "Automatic Segmentation and Reconstruction of the Cortex from Neonatal MRI," Neuroimage, Vol. 38, No. 3, pp. 461-477, 2007.
- [5] J. K. Udupa, D. Odhner, A. X. Falcao, K.C. Ciesielski, P. A. V. Miranda, P. Vaideeswaran, S. Mishra, G. J. Grevera, B. Saboury and D. A. Torigian, "Fuzzy Object Modeling," SPIE Proceedings, Medical Imaging 2011, Vol. 7964, 79640B-1-10, 2011.
- [6] S. Kobashi and J. K. Udupa, "Fuzzy Object Models for Newborn Brain MR Image Segmentation," SPIE Proceedings, Medical Imaging 2013, Vol. 8672, 2013.
- [7] B. C. Davis, P. T. Fletcher, E. Bulitt and S. Joshi, "Population Shape Regression From Random Design Data," Proc. of IEEE 11th Int. Conf. on Computer Vision, pp. 1-7, 2007.
- [8] P. Aljabar, R. Wolz, L. Srinivasan, S. Counsell, J. P. Boardman, M. Murgasova, V. Doria, M. A. Rutherford, A. D. Edwards, J. V. Hajnal and D. Rueckert, "Combining Morphological Information in a Manifold Learning Framework: Application to Neonatal MRI," Lecture Notes in Computer Science, Medical Image Computing and Computer-Assisted Intervention, Vol. 6363, pp. 1-8, 2010.
- [9] M. belkin and P. Niyogi, "Laplacian Eigenmaps for Dimensionality Reduction and Data Representation," Neural Computation, Vol. 15, No. 6, pp. 1373-1396, 2003.
- [10] E. Remy and E. Thiel, "Computing 3D Medial Axis for Chamfer Distance", Lecture Notes in Computer Science Vol.1953, pp.418-430, 2000.
- [11] L.B.Lusted, "Single detectability and medical decision making.", Science 171, pp.1217-1219, 1971.